

Integrating Input from Multiple Signals: The VirA/VirG Two-Component System of *Agrobacterium tumefaciens*

Aindrila Mukhopadhyay, Rong Gao, and David G. Lynn^{*[a]}

Bacteria, fungi, and plants exploit histidine sensor kinase/response regulators to mobilize complex responses to inputs as diverse as environmental stimuli and hormonal regulation. More than 50 such two-component systems are found in many organisms, yet the mechanisms of signal perception, phosphotransfer regulation, and even the nature of the activating signals remain poorly defined. Here we resolve each phosphate transfer event in vivo for the Agrobacterium tumefaciens virulence two-component system VirA/VirG. The input signals for this system are known, and the complex autocatalytic regulation of the signaling

components has been removed. Two separate and independent phosphotransfer events are resolved, an initial ATP→sensorHis~PO₄→receiver~PO₄ that may be activated by xenogostic sugar/low pH, and a subsequent ATP→His~PO₄→VirG~PO₄ that requires xenogostic phenol activation. The identification of these separate pathways places biochemical limits on the regulated steps in this two-component signal transduction module and further extends the model of how a single sensor is able to integrate multiple input stimuli.

Introduction

Agrobacterium tumefaciens successfully induces crown gall tumors in hundreds of host species.^[1–3] The signals that mediate host perception, the process of xenogostic, must be both sufficiently specific to ensure precise host commitment and yet appropriately general to detect multiple hosts. These complex requirements leading to tumorigenesis are apparently regulated by a single VirA/VirG two-component signaling system. VirA, the sensor kinase, responds cooperatively to three separate signals, phenols (for example, acetosyringone (AS)), monosaccharides (via the periplasmic sugar-binding protein ChvE)^[4,5] and acidic pH, to control both the rate and magnitude of virulence (*vir*) gene induction.^[6–10] While models for the activation of response regulators such as VirG have been proposed (for reviews see refs. [11–13]), and signal-dependent phosphorylation have been demonstrated for several systems in vivo,^[14–17] the mechanism of signal perception, sensor activation, and cascade regulation in two-component systems remain an area of active investigation.^[18–21]

The ability of VirA to integrate three separate input signals makes it one of the more complex sensor/transmitters. Nevertheless, several features make this system suitable for more detailed analysis. The structurally defined input signals have enabled mechanistic models for signal perception to be developed.^[8,16,22] Several mutant alleles that alter both signal perception^[23–25] and transmission^[22] are known. The complications presented by signal-dependent expression of *virA* and *virG*^[26–30] have been addressed with the constitutive T5 phage promoter *P*_{N25}, successfully decoupling VirA/VirG expression from signal activation.^[31] Moreover, these constructs have allowed the attachment of affinity tags to active alleles for rapid isolation of proteins with labile ³²P phosphates directly from bacterial cultures. Finally, autophosphorylation of a His474 of the kinase domain of VirA and the phosphotransfer to the Asp52 residue

of VirG have been demonstrated in vitro.^[16,32,33] Here we report evaluation of the entire phosphorylation cascade in vivo and reveal two separate phosphotransfer pathways. These two pathways may be regulated by separate input signals; this explains much of the genetic evidence for the response to multiple inputs. However, it is also possible that a single ratcheting mechanism^[22] operates to transmit all signal inputs.

Results

In vivo phosphorylation of VirG

The native *virG* promoter in *Agrobacterium* is under complex regulation^[27,28,30] and pYW48, containing *P*_{N25}-6XHis-*virG* and *virA*, was constructed to decouple *virG* expression from signal activation.^[31] As shown in Figure 1A, *vir* gene expression in the pTi-cured A136 background containing pYW48 and the reporter construct pSW209 (*P*_{virB}:*lacZ*) was similar to that of the A348 control containing wild-type promoters of *virG* and *virA*. Neither constitutive expression of *virG* nor addition of the N-terminal 6XHis-tag significantly altered VirG function.

For in vivo phosphorylation, A136 strains carrying pYW48 were phosphate starved overnight in induction media, then pulsed with H₃³²PO₄, and AS (200 μM) was added at progressively later times during the labeling period. The 6XHis tagged VirG was affinity enriched by Ni-resin purification. As can be seen in Figure 1B, phosphate labeling could be detected as

[a] Dr. A. Mukhopadhyay, R. Gao, Prof. Dr. D. G. Lynn
Center for Fundamental and Applied Molecular Evolution
Department of Chemistry and Biology, Emory University
Atlanta, GA 30322 (USA)
Fax: (+1) 404-727-6586
E-mail: david.lynn@emory.edu

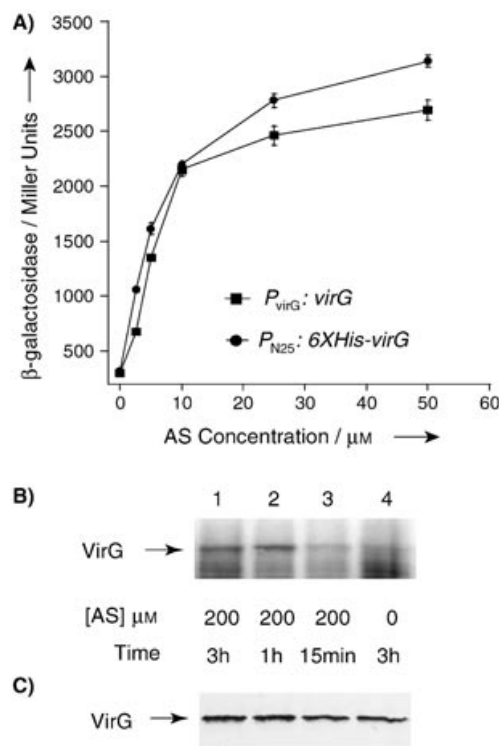


Figure 1. A) *vir* gene expression via $P_{\text{N25}}::6\text{XHis-virG}$. Activation of P_{virB} was measured in terms of β -galactosidase activity by using the reporter construct $P_{\text{virB}}::\text{lacZ}$ (*pSW209*) after 8 h of cocultivation with indicated AS concentrations in *Agrobacterium* strains (■) A348(*pSW209*), containing $P_{\text{virG}}::\text{virG}$, and (●) A136(*pSW209/pYW48*), containing $P_{\text{N25}}::6\text{XHis-virG}$. Both strains contain native *virA*. Each concentration represents triplicate analyses expressed as \pm SD. B) Effect of AS induction on the phosphorylation of VirG in vivo. Phosphorimage of Ni-resin enriched 6XHis-VirG from *A. tumefaciens* strain carrying *pYW48* radiolabeled with $\text{H}_3^{32}\text{PO}_4$ ($30 \mu\text{Ci mL}^{-1}$) in the presence of AS (200 μM) for progressively shorter time periods of 3 h (lane 1), 1 h (lane 2), 15 min (lane 3) and without AS for 3 h (lane 4). C) anti-RGSHis immunoblot analysis of the blot shown in panel B.

early as 15 minutes after AS exposure, reached a maximum within 1 h, and did not increase significantly over 3 h. Without AS, no significant $\text{VirG}\text{-}^{32}\text{P}$ accumulates in vivo (Figure 1B, lane 4), even though equivalent quantities of the 6XHis-VirG protein are present (Figure 1C, lane 4).

To further examine the AS dependence of VirG phosphorylation, a simple analogue of the natural MDIBOA inhibitor of *vir* gene induction,^[34] hydroxy furanone (HF) was employed as an inhibitor. As shown in Figure 2A, 100 μM HF completely inhibits *vir* gene induction by 100 μM AS. Likewise, HF inhibits accumulation of $\text{VirG}\text{-}P$ under the same conditions (Figure 2B).

Role of VirA in VirG phosphorylation

Agrobacterium strains carrying a *VirA*(G665D) allele^[25] are leaky and show basal *vir* expression that is further elevated with AS induction (Figure 3A). Likewise, strains containing *VirA*(G665D) show phosphate accumulation without AS induction (Figure 3B, lane 4), and the level of phosphorylation increases with

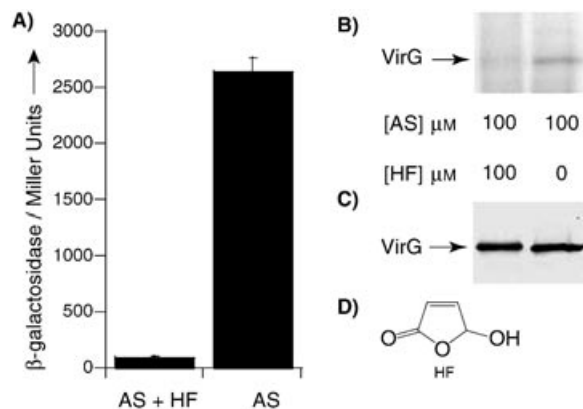


Figure 2. Effect of inhibitors on the accumulation of $\text{VirG}\text{-}P$ in vivo. A) *A. tumefaciens* carrying *pYW48* was assayed for *vir* gene induction ($P_{\text{virB}}::\text{lacZ}$, *pSW209*) after 8 h in 100 μM AS, with or without 100 μM HF. B) Phosphorimage of the Ni-resin purified 6XHis-VirG from bacterial cultures radiolabeled with $\text{H}_3^{32}\text{PO}_4$ for 3 h with either 100 μM AS and 100 μM HF (lane 1) or with 100 μM AS alone (lane 2). C) anti-RGSHis immunoblot analysis of the blot shown in panel B. D) Molecular structure of hydroxy furanone (HF).

AS induction (lane 5). The level of phosphorylation in both wild-type and mutant strains (lanes 1–3) is in qualitative agreement with the observed *vir* gene expression.

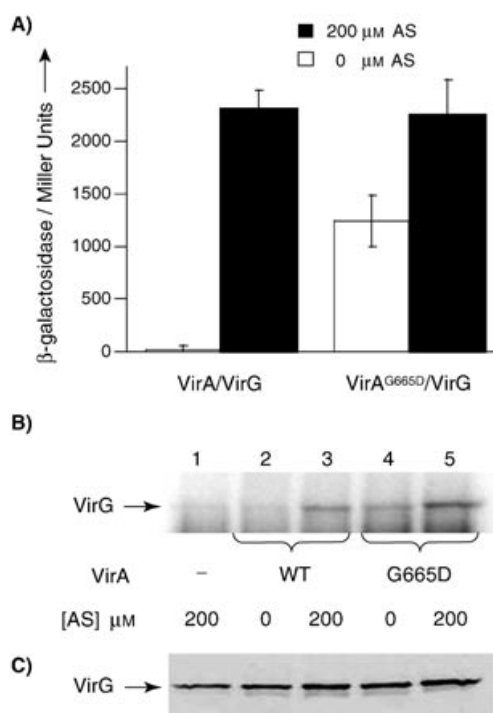


Figure 3. Role of *VirA* in *vir* gene induction and $\text{VirG}\text{-}P$ phosphorylation. A) Expression of $P_{\text{virB}}::\text{lacZ}$ (*pSW209*) was measured after 16 h of co-cultivation with (filled bar) or without (open bar) 100 μM AS in A136 containing *virA* (*pYW48*) or *virA*(G665D) (*pAM30*) and $P_{\text{N25}}::6\text{XHis-virG}$. B) Phosphorimage of Ni-resin enriched 6XHis-VirG from $\text{H}_3^{32}\text{PO}_4$ radiolabeled (3 h) *A. tumefaciens* strains carrying *pYW47* (-*VirA*) with 200 μM AS (lane 1), *pYW48* without AS (lane 2), *pYW48* with 200 μM AS (lane 3), *pAM30* (*VirA*^{G665D}) without AS (lane 4) 200 μM AS, and *pAM30* (*VirA*^{G665D}) with 200 μM AS (lane 5). C) anti-RGSHis immunoblot analyses of the blot shown in panel B.

The VirG phosphoprotein

Both homology modeling^[35] and mutagenesis^[32] experiments suggest D52 as the site of phosphorylation in VirG. The hydrolytic instability of such acyl phosphates, particularly under base and acid catalysis, is well known^[36] and can be employed as a chemical test. Accordingly, Ni-resin-enriched fractions from labeled bacteria were resolved by SDS-PAGE, transferred to PVDF membranes and treated with either 1 N HCl or 3 N NaOH for 45 minutes at room temperature prior to phosphorimaging. As shown in Figure 4A, the VirG~P was stable under neutral con-

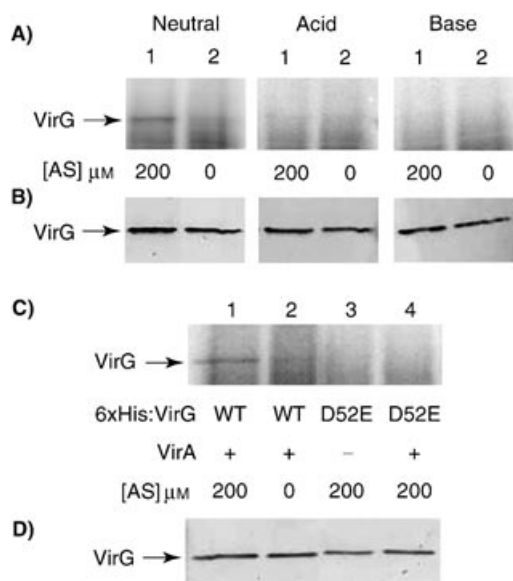


Figure 4. A) Chemical stability of VirG~P. Three equivalent PVDF membranes with Ni-resin enriched 6XHis-VirG from *A. tumefaciens* strain A136 carrying pYW48 radiolabeled with $H_3^{32}PO_4$, either in the presence (lane 1 in each) or the absence (lane 2 in each) of 200 μM AS, were treated with either TBS at pH 7.0 (neutral), 1 N HCl (acid), or 1 N NaOH (base) for 1 h at room temperature prior to phosphorimaging. B) anti-RGSHis immunoblot analyses of the blot shown in panel A. C) *in vivo* phosphorylation of VirG^{D52E}. Phosphorimage of Ni-resin enriched 6XHis-VirG from A136 carrying pYW48 radiolabeled with $H_3^{32}PO_4$ for 3 h with 200 μM AS (lane 1) or without AS (lane 2) and compared with enriched fractions from A136 carrying either pAM19 (VirG^{D52E}, -VirA) with 200 μM AS (lane 3) or pAM21 (VirG^{D52E}, +VirA) with 200 μM AS (lane 4). D) anti-RGSHis immunoblot analyses of the blot shown in panel C.

ditions, but both acid and base hydrolyzed the $^{32}PO_4$ while not significantly removing the protein from the membrane (Figure 4B).

To evaluate the site of phosphorylation, *Agrobacterium* strains carrying P_{N25} -6XHis-*virG* (D52E) were constructed with (pAM21) and without (pAM19) *virA*. The D52E substitution represents a very conservative change, but one known to disable *vir* gene expression.^[37] Consistent with the functional analysis, the D52E allele did not accumulate phosphate (Figure 4C, lanes 3 and 4) with AS-induced VirA.

In vivo phosphorylation of VirA

In addition to autocatalytic *virA* expression with signal induction^[27] and the chemical instability of His~P intermediates, the

membrane localization of VirA further complicates *in vivo* labeling protocols. Since the C-terminal cytoplasmic portion of VirA retains the ability to respond to AS induction,^[38,39] a P_{N25} -6XHis-*virA*(aa285–829) construct was generated in pYW21 (Figure 5A, Table 1). Consistent with the wild-type protein, strains

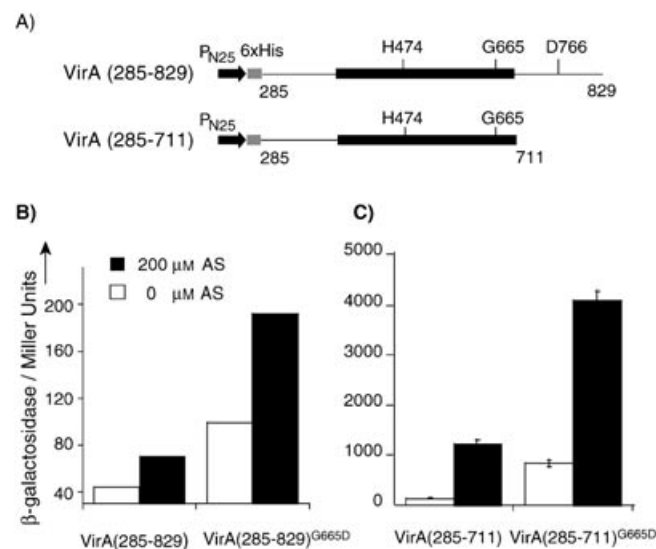


Figure 5. *vir* gene expression with P_{N25} -6XHis-*virA* constructs. A) Physical maps of VirA(aa285–829), VirA(aa285–829)(G665D), VirA(aa285–711), and VirA(aa285–711)(G665D) used in *A. tumefaciens* strain A348–3 ($\Delta virA$, and *Ti* plasmid-borne *virG*). B) Activation of P_{vir} was measured in terms of β -galactosidase activity by using the reporter construct $P_{vir8}::lacZ$ (pSW209 Ω) after 16 h of cocultivation without AS (open bar) or with 100 μM AS (filled bar) in *Agrobacterium* strains containing broad-host-range vector-borne P_{N25} -6XHis-*virA*(aa285–829) (pYW21) or P_{N25} -6XHis-*virA*(aa285–829)(G665D) (pYW39). C) β -Galactosidase activity measured as in B), in *Agrobacterium* strains containing broad-host-range vector-borne P_{N25} -6XHis-*virA*(aa285–711) (pAM28) or P_{N25} -6XHis-*virA*(aa285–711)(G665D) (pAM23).

carrying pYW21 remained fully AS dependent, even though removal of the periplasmic domain eliminated cooperative sugar activation and reduced maximal activity (Figure 5B). In alleles carrying the G665D substitution,^[25] the constitutive basal *vir* expression was still further induced by AS.

VirA belongs to a family of hybrid sensor kinases that contain an additional C-terminal domain, aa711–829, which is homologous to the receiver of response regulators. Deletion of the receiver domain from VirA^{wt} increases basal activity.^[38,40] As shown in Figure 5C, the basal *vir* gene expression with VirA(aa285–711) (pAM28) was also further induced by AS. Moreover, in strains expressing VirA(aa285–711)(G665D) (pAM23), *vir* gene expression was comparable to that achieved with full length VirA^{wt} in the presence of glucose (Figure 3A). Removal of the VirA-receiver domain therefore at least partially complements the loss of sugar/pH synergistic activation.

VirA(aa285–829) is phosphorylated *in vivo* with or without AS (Figure 6A, lanes 1 and 2). This phosphate accumulation increases with AS induction in both VirA(aa285–829) and in alleles carrying the G665D substitution. The relative amount of phosphate accumulation is justified relative to Western analysis

Table 1. Bacterial strains and plasmids.

Strain/ plasmid	Relevant characteristics	Ref.
<i>E. coli</i>		
XL1-Blue	<i>recA1 endA1 gyrA96 thi-1 hsdR17 supE44 relA1 lac[F' proAB lacIqZ M15 Tn 10(Tc^r)]</i>	Stratagene
XL10-Gold	<i>Tc^r(mcrA)183 (mcrCB-hsdSMR-mrr)173 endA1 supE44 thi-1 recA1 gyrA96 relA1 lac Hte [F' proAB lacIqZM15 Tn10 (Tc^r) Amy CamR]</i>	Stratagene
<i>A. tumefaciens</i>		
A136	Strain C58 cured of pTi plasmid, Rif ^r , Nal ^r	[51]
A348-3	A136 containing pTiA6NC, Δ <i>P</i> _{virA} - <i>virA</i>	[16]
Plasmids		
PCR2.1	TA cloning vector, ColE1, Ap ^r	Invitrogen
pVRA8	<i>P</i> _{virA} - <i>virA</i> ^{WT} from pTiA6 in pUCD2, pBR322ori, IncW, Ap ^r /Km ^r /Spec ^r	[16]
pMutA	<i>P</i> _{virA} - <i>virA</i> ^{G665D} in pUCD2, pBR322ori, IncW, Ap ^r /Km ^r /Spec ^r	[25]
pYW47	<i>P</i> _{N25} -6xHis- <i>virG</i> in pYW15b, Ap ^r	[31]
pYW48	4.5 Kb <i>KpnI</i> fragment containing <i>P</i> _{virA} - <i>virA</i> cloned into pYW47, Ap ^r	[31]
pGP408	750bp fragment containing <i>virG</i> ^{D52E} Ap ^r	[a]
pAM19	<i>P</i> _{N25} -6xHis- <i>virG</i> ^{D52E} in pYW15b, Ap ^r	this study
pAM21	4.5 Kb <i>KpnI</i> fragment containing <i>P</i> _{virA} - <i>virA</i> cloned into pAM19, Ap ^r	this study
pYW21	<i>P</i> _{N25} -6xHis- <i>virA</i> (aa258–829) in pYW15b, Ap ^r	[39]
pYW39	<i>P</i> _{N25} -6xHis- <i>virA</i> (aa258–829)(G665D) in pYW15b, Ap ^r	[31]
pYW45	<i>P</i> _{N25} -6xHis-LZ- <i>virA</i> (aa258–829) in pYW15b, Ap ^r	[39]
pAM22	<i>P</i> _{N25} -6xHis-LZ- <i>virA</i> (aa258–711) in pYW15b, Ap ^r	this study
pAM23	<i>P</i> _{N25} -6xHis- <i>virA</i> (aa258–711)(G665D) in pYW15b, Ap ^r	this study
pAM28	<i>P</i> _{N25} -6xHis- <i>virA</i> (aa258–711) in pYW15b	this study
pAM30	4.5 Kb <i>KpnI</i> fragment containing <i>P</i> _{virA} - <i>virA</i> ^{G665D} cloned into pYW47, Ap ^r	this study
pRG90	<i>P</i> _{N25} -6xHis-LZ- <i>virA</i> (aa258–829)(H474Q) in pYW15b, Ap ^r	this study
pRG110	<i>P</i> _{N25} -6xHis-LZ- <i>virA</i> (aa258–829)(D766N) in pYW15b, Ap ^r	this study
pSW209	<i>P</i> _{virB} - <i>lacZ</i> fusion derived from pSW243 cd, IncP, Km ^r	[b]
pSW209Ω	Truncated version of pSW209, IncP, Spec ^r , Km ^r	[31]

[a] A. Das, University of Minnesota (USA). [b] S. C. Winans, Cornell University (USA).

(data not shown) as well as to background phosphorylation (e.g., see band 1).

The VirA phosphoprotein

The remaining panels of Figure 6 compare the acid and base sensitivity of phospho-VirA(285–829). As shown in Figure 6C, mild base treatment removes the VirA phosphate that accumulates without AS induction (lane 2). In contrast, this phosphate is partially resistant to acid treatment (Figure 6B, lane 2). The additional phosphate accumulation induced by AS (Figure 6B, lanes 1 and 3) or in the constitutive G665D alleles (Figure 6B, lanes 3 and 4), is removed by acid treatment; this results in equivalent amounts of phosphate remaining for all four VirA samples. An identical membrane washed sequentially, first under acidic then basic conditions, lost all accumulated phosphate (Figure 6D). These data suggested that a mixture of

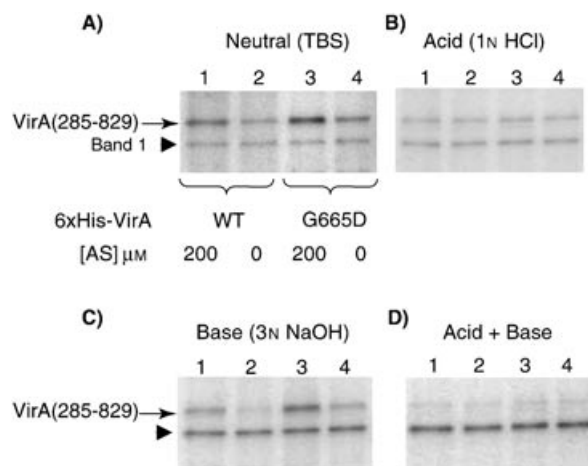


Figure 6. In vivo phosphorylation of VirA(aa285–829). Four identical PVDF membrane blots containing Ni-resin enriched fractions from radiolabeled ($25 \mu\text{Ci H}_3^{32}\text{PO}_4\text{mL}^{-1}$ for 2.5 h) *A. tumefaciens* strains carrying broad-host-range vector-borne *P*_{N25}-6xHis-*virA*(aa285–829) (pYW21) with 200 μM AS (lane 1) or without AS (lane 2) and *P*_{N25}-6xHis-*virA*(aa285–829)(G665D) (pYW39) with 200 μM AS (lane 3) or without (lane 4), in each panel and treated with either A) TBS at pH 7.0 (neutral), B) 1 N HCl (acid), C) 3 N NaOH (base), or D) sequentially with acid and base prior to phosphorimage analyses.

acid-labile and base-labile phosphates exist in AS-induced VirA(aa285–829).

Reasoning that the receiver domain might contain a phosphorylated site, the VirA(aa285–711) and VirA(aa285–711)(G665D) alleles were constructed. Phosphate accumulation in these alleles mirrored that seen in VirA(aa285–829), both with respect to the G665D substitution and AS induction (Figure 7A). However, the base labile phosphate could no longer be detected (Figure 7C), and all the accumulated phosphate was completely removed by acid treatment alone. Such acid

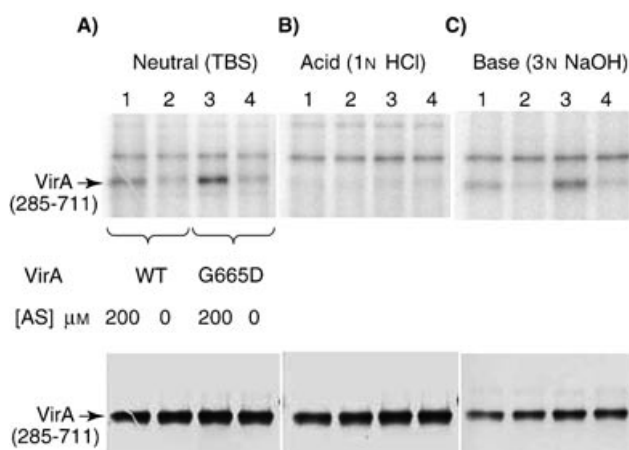


Figure 7. In vivo phosphorylation of VirA(aa285–711). Three identical PVDF membrane blots containing Ni-resin enriched fractions from $\text{H}_3^{32}\text{PO}_4$ radiolabeled *A. tumefaciens* strains carrying *P*_{N25}-6xHis-*virA*(aa285–711) (pAM28) with 200 μM AS (lane 1) or without AS (lane 2) and *P*_{N25}-6xHis-*virA*(aa285–711)(G665D) (pAM23) with 200 μM AS (lane 3) or without AS (lane 4), in each panel and treated with either A) TBS at pH 7.0 (neutral), B) 1 N HCl (acid), or C) 3 N NaOH (base). Anti-RGSHis immunoblot analyses of the blots in A, B, and C are shown in the corresponding lower panels.

lability and base stability is uniquely characteristic of His~P. Based on receiver homology comparisons, the partial acid stability and base lability of the other phosphate in VirA(aa285–829) was anticipated to be the D766 acyl phosphate but neither hydroxyl amine nor borohydride treatments were found that could remove the phosphate.

Site-specific substitutions were introduced into the more stable leucine zipper fusion constructs reported previously (Figure 8).^[22] Alleles carrying the H474Q substitution show no accumulation of phosphate (Figure 8B, lane 1); this suggests that initial phosphorylation is dependent on initial H474 phosphorylation. Alleles carrying the D766N substitution, however, still accumulate phosphate; this further suggests that D766 is not the residue that receives the phosphate from H474.

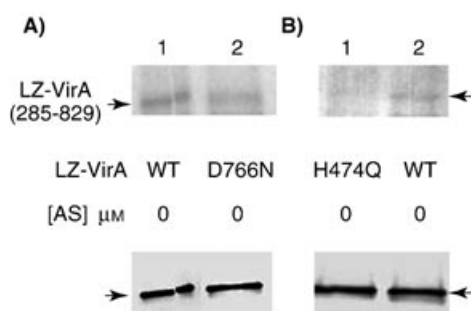


Figure 8. In vivo phosphorylation of LZ-VirA(aa285–829) without AS. Phosphorimage of Ni-resin enriched fractions from $H_3^{32}PO_4$ -labeled *A. tumefaciens* strains carrying indicated LZ-VirA constructs. A) Lanes: 1: pYW45, LZ-VirA(aa285–829); 2: pRG110, LZ-VirA(aa285–829)(D766N). B) Lanes: 1: pRG90, LZ-VirA(aa285–829)(H474Q); 2: pYW45, LZ-VirA(aa285–829). Anti-RGSH immunoblot analyses are shown in the corresponding lower panels.

Discussion

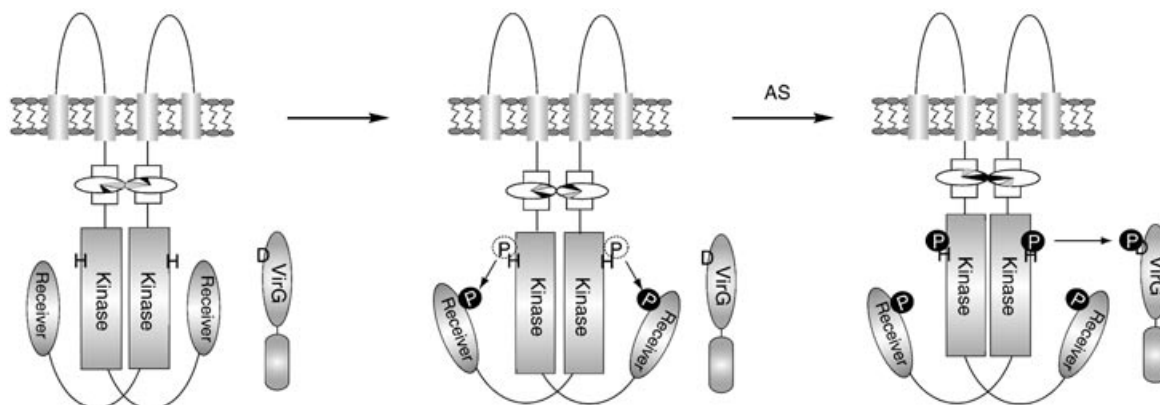
The modularity of the sensor-transmitter/response regulator proteins probably contributed to the extraordinary number and variety of these input/output (I/O) modalities.^[11] VirA, for example, tolerates radical domain truncation, and many of the individual domains retain function when expressed individual-

ly.^[29,38] Moreover, these apparently simple two-component signal-transduction systems can be both specific and tightly regulated. The acyl~P of VirG forms in vivo only under appropriate inducing conditions, and natural and synthetic inhibitors of *vir* gene expression inhibit VirG phosphorylation. The simple addition of one more methylene in VirG(D52E) prevents phosphorylation.

The VirA/VirG system is, however, distinctive among these systems for two reasons. First, it integrates multiple input signals—maximal induction requires acidic pH, monosaccharides, and phenols. Second, VirA carries an additional receiver domain at its C terminus. We show here that the cytoplasmic VirA(aa285–829) constitutively autophosphorylates in vivo, independently of the presence of xenonostic phenol AS, and this phosphorylation requires the C-terminal receiver domain.

In previous studies, analysis of in vivo phosphorylation in a eukaryotic histidine sensor kinase homologue, DokA, which also contains a receiver domain, revealed a signal-dependent phosphorylation on a serine residue.^[18] Like acyl phosphates, serine phosphates in proteins are labile to mild base treatment. However, serine phosphates are generally acid stable, while acyl phosphates are known to be partially or completely hydrolyzed under acidic conditions,^[41] much as was seen here for VirG. The VirA~P formed in the absence of AS displayed partial sensitivity to acid, more consistent with an acyl phosphate, but neither borohydride or hydroxyl amine treatments removed the phosphate. Moreover, VirA(285–829) alleles carrying a D766N mutation (the conserved aspartate in the receiver domain) do autophosphorylate, but are inactive in vivo. Therefore D766, though functionally required,^[38] appears not to serve as a site of phosphorylation. Finally, the VirA(aa285–829) allele carrying a H474Q mutation at the conserved histidine residue in the kinase domain does not autophosphorylate and is not functional in inducing *vir* gene expression. Taken together, these results are most consistent with an ATP→H474~PO₄→receiver domain phosphotransfer that operates constitutively in VirA(aa285–829) (Scheme 1).

This internal phosphotransfer pathway is not sufficient to induce VirG phosphorylation. Rather, VirA(aa285–829) accumulates histidyl phosphate only under inducing conditions; this



Scheme 1. Model for the AS-mediated activation of the VirA/VirG two-component system.

results in multiple phosphorylations of VirA *in vivo*. Strains carrying the G665D alleles show constitutive histidine phosphorylation that is further elevated by AS induction. Therefore, an independent sensor/response regulator phosphotransfer pathway, $\text{ATP} \rightarrow \text{VirA-H474-PO}_4 \rightarrow \text{VirG-D52-PO}_4$, requires xenonostic phenol activation (Scheme 1).

Previous genetic analyses of signal-induced activation in VirA are consistent with these two phosphotransfer pathways. It has been suggested that the receiver module interacts with the kinase module to repress its activity,^[29] and phosphorylation of the receiver could relieve this repression. Thus, the phenol-independent receiver phosphorylation pathway appears to be necessary for optimal *vir* gene expression while the phenol induced $\text{ATP} \rightarrow \text{VirA-H474-PO}_4 \rightarrow \text{VirG-D52-PO}_4$ pathway is indispensable. Interestingly, synergistic signals, such as sugars and low pH, are also known to be necessary, but not sufficient to induce *vir* gene expression without phenol in wild-type strains. Deletion of the VirA receiver domain causes drastic lowering in this synergistic effect of sugars.^[29,38] These results are consistent with a model that sugar/ChvE^[4] regulates phosphorylation of the terminal receiver domain of VirA,^[42] that is, the first step in Scheme 1. ChvE, a periplasmic sugar-binding protein, was found to mediate monosaccharide sensing in VirA. Interaction of a ChvE/sugar complex with the periplasmic domain could then result in some piston/tilt/rotation motion in the transmembrane regions that transmits through the cytoplasmic domains to activate phosphorylation of the VirA receiver. Truncation of the periplasmic domain may deregulate this pathway and allow VirA(aa285–829) to phosphorylate the receiver constitutively. However, it is not clear whether the level of this constitutive phosphorylation is sufficient to completely relieve repression by the receiver domain.

Some hybrid histidine kinases, for example, Sln1p, BvgS, employ a multistep phosphorelay through additional receiver domains to allow integration of multiple signals at the intermediate step.^[43,44] However, there is no indication that a similar phosphorelay mechanism exists in the VirA/VirG system.

Following previous leucine-zipper fusion strategies developed in chemotaxis systems,^[45] we showed that the dimer interface for the predicted coiled coils within the phenol signal-input domain of VirA can adopt active, inactive, and partially active dimer interfaces.^[22] We concluded that activity is defined by the relative orientation, or phase, of the coiled-coil interface. Others have also found critical coiled coils within input domains and argued for a role of these regions in kinase activation.^[46–48] Therefore, an alternate explanation for VirA activation requires all inputs—sugar, pH, and phenol—to be transmitted via a “ratcheted” access to the most active coiled-coil interface. By this analysis, removal of the periplasmic domain allows access to a coiled-coil conformation that activates VirA receiver phosphorylation, and phenol exposure drives access to a conformation capable of phosphorylating VirG. While the precise role of D766 and the exact residue that receives the phosphate have yet to be determined, this model places full responsibility for signal propagation on the linker domain. The degree of coupling between these two inputs remains an important area for further investigation.

As functionally modular as the VirA protein appears, input responses remain complex and sensitive to environmental conditions. For example, isolation of VirA as inner-membrane preparations^[16] removes the requirement for xenogonin-induced phosphorylation. The extent to which this responsiveness is modulated by other proteins, as in the case of ChvE, or simply a reflection of the “hair trigger” of the conformations of this signal integrator needs to be resolved. Nevertheless, the ability of VirA/VirG to integrate three separate inputs certainly provides critical information for this pathogen, and understanding its mechanisms may allow these multi-input benefits to be extended into other molecular I/O applications.

Experimental Section

Bacterial strains and plasmids: Strains and plasmids are shown in Table 1. *A. tumefaciens* strains were grown in LB medium or AB minimal medium at 28 °C. *E. coli* strains were grown in LB medium at 37 °C and used as the cloning host.

Construction of expression vectors: Construction of pYW47 and pYW48 is described in previous work.^[31] For pAM19, DNA that encodes amino acids 2–300 of VirG^{D52E} was amplified by PCR from the encoding plasmid, pGP408, by using primers A-GON, 5'-GGGGTACCTCAGGCTGCCATCGTCCC-3' (*KpnI*), and S-GON, 5'-GGGAGCTCAAACAGTCTTCTTATC-3' (*SacI*). PCR products were cloned into the PCR2.1 vector (Invitrogen) as per the manufacturer's instructions, and plasmid transformation into *E. coli* strains followed a heat-shock protocol with XL1-blue competent cells (Stratagene). The D52E mutation introduces a *SacI* restriction site in the *virG* *orf*, hence a partial digestion with *SacI* followed by a complete *KpnI* digest was used to obtain the 750 bp *virG* *orf*. The desired fragment was released and cloned into the corresponding sites in the multicloning site (MCS) of pYW15b to give plasmid pAM19. The 4.5 Kb *KpnI* *P*_{virA}-*virA* fragment from pVRA8 was cloned into pAM19 to give pAM21, and the 4.5 Kb *KpnI* *P*_{virA}-*virA*(G665D) fragment from pMutA was cloned into pYW47 to create pAM30. Construction of vectors containing the C terminus cytoplasmic domains of *virA*, that is, VirA(aa285–829), VirA(aa285–829)(G665D), and LZ-VirA(aa285–829) have been reported previously.^[22] In this study, similar constructs of *virA* with the receiver domain truncated, that is, VirA(aa285–711), were generated by using site-specific mutagenesis designed to introduce a STOP codon at the position corresponding to aa712 of *virA*. Amplification of the entire vector was carried out using *pfu* polymerase (Stratagene). Overlap primers 5'-AATAAGGCACCGCGTTGAAACGGGGAGATTGTG-3', and 5'-CACAACTCCCGGTTCAACGCGGTGCCTTATTT-3', were used to introduce a single nucleotide mutation in the *orf* of *virA* to give a STOP codon at the aa712. The PCR protocol used 100 ng template DNA, 10 pmol of each primer. The PCR product mixture was treated with *DpnI* for 2 h at 37 °C to completely digest the original template DNA. 3 μL of the resulting PCR mix was used to transform Ultra competent XL10-gold cells via heat shock. Transformed colonies were analyzed by restriction digestion of isolated plasmids as well by IPTG induction to examine expression and size of proteins. STOP codon incorporation in pYW45 and pYW39 led to the generation of pAM22 encoding *P*_{N25}-6XHis-LZ-*virA*(aa285–711) and pAM23 encoding *P*_{N25}-6XHis-*virA*(aa285–711)(G665D) respectively. An internal *HindIII* site in the *virA* *orf* was used along with the *HindIII* site in the MCS downstream of *virA* to digest pAM22. The *HindIII* fragment from pAM22 containing the STOP codon was

ligated into pYW39 digested with *Hind*III to generate pAM28, encoding $P_{N25-6XHis-virA}$ (aa285–711).

Plasmid DNA was isolated with QIAprep spin columns (Qiagen) and plasmid constructs were confirmed by restriction-digestion analysis. Restriction enzymes and T4 DNA ligase were obtained from Promega or New England Biolabs. Plasmid transformation into *Agrobacterium* was achieved with a Gene pulser and a 0.2 cm electroporation cuvette (Bio-rad) at 2.5 KV, 400 Ω , and 25 KF. Electrocompetent *Agrobacterium* cells were prepared as described previously.^[49]

vir gene induction: pSW209 and pSW209 Ω carry the β -galactosidase reporter construct $P_{virB}::lacZ$ and were used to assay *vir* gene expression in *Agrobacterium*. Bacteria were grown in 20 mL of LB medium to an OD₆₀₀ 0.4–0.6 mL⁻¹ in the presence of the appropriate antibiotics. The bacterial cell mass was harvested by centrifugation for 10 minutes at 7000g and 4°C. The pellet was diluted to an OD₆₀₀ of ~0.1 mL⁻¹ into tubes containing a total of 1 mL induction medium (I.M.),^[49] and this was cultured at 28°C with shaking at 225 rpm. β -Galactosidase activity was determined as described by Miller.^[50] For concentration-dependent *vir* gene induction assay, indicated quantities of AS were used, and the cultures were assayed after the indicated induction period (usually 16 h). For inhibition assays with hydroxy furanone (HF, Fluka), I.M. with 1% glycerol was used as carbon source.

In vivo protein phosphorylation: Overnight cultures (15 mL) of the various *Agrobacterium* strains were grown in LB media containing appropriate antibiotics to an OD₆₀₀ of 0.4–0.8 mL⁻¹. The bacteria were harvested at 7000g and 4°C. Overnight phosphate starvation was performed by resuspending bacteria at an OD₆₀₀ of 0.15 mL⁻¹ in phosphate-deficient I.M. (15 mL, per liter: 3.9 g MES hydrate, 50 mL of 20x AB salts,^[49] 1% glucose, (or 1% glycerol for inhibition experiments with HF)) with appropriate antibiotics. After 12 h of phosphate starvation, H₃³²PO₄ (NEN Dupont) was added at a specific activity of 40 μ Ci mL⁻¹, and the phenolic inducer, aceto-syringone (AS) was added as indicated. Labeling was allowed to proceed for the indicated time intervals before the bacteria were harvested at 4°C for 10 min at 7000g. They were then resuspended in denaturing lysis buffer (1 mL, at pH 7.6, Qiagen), and lysed by sonication on ice for 30 s with microtip pulses at 28% of 600 W (ColeParmer 600 W Ultrasonic Homogenizer). The lysate was clarified by centrifugation at 13000g, and the supernatant used in Ni-resin purification as per the Qiagen protocol for denatured proteins by using modified denaturing wash (with 25 mM imidazole, pH 7.5) and elution (with 500 mM imidazole, pH 8.6) buffers. The eluants were resolved by SDS-PAGE (Novex, 14% for VirG, 10–12% for VirA) and electro-blotted (Trans-blot, Bio-rad) onto nitrocellulose (Bio-rad) or PVDF (NEN Dupont) membranes for visualization by phosphorimaging and immunoblot (Western) analyses.

Immunoblot analyses: To detect the 6XHis-tagged proteins, the electro-blotted nitrocellulose (BioRad) or PVDF (NEN Dupont) membranes were probed first with anti-RGSHis monoclonal Ab (Qiagen) at 1:200 dilution. Visualization was achieved by using alkaline phosphatase-conjugated rabbit-anti-mouse secondary antibody (Pierce), 1:1000 dilution, followed by 1-Step NBT/BCIP (Pierce) developing.

Analysis of phosphoprotein chemical stability: A set of equivalent electroblotted PVDF membranes was incubated at room temperature for 45 min to 3 h in either 3 N NaOH (base), 1 N HCl (acid), or TBS at pH 7 (control), washed with TBS, dried and evaluated by phosphorimaging.

Acknowledgements

We are grateful to the National Institutes of Health for support (grant GM47369) and to Professor Andrew Binns and Arlene Wise for careful reading of this manuscript.

Keywords: pathogenesis • phosphorylation • signal transduction • two-component system • VirA

- [1] J. D. Heath, T. C. Charles, E. W. Nester in *Two-Component Signal Transduction* (Eds.: J. Hoch, T. J. A. Silhavy), ASM Press, Washington, DC, **1995**, pp. 367–386.
- [2] J. Zhu, P. M. Oger, B. Schrammeijer, P. J. Hooykaas, S. K. Farrand, S. C. Winans, *J. Bacteriol.* **2000**, *182*, 3885–3895.
- [3] T. Tzfira, V. Citovsky, *Trends Cell Biol.* **2002**, *12*, 121–129.
- [4] G. A. Cangelosi, R. G. Ankenbauer, E. W. Nester, *Proc. Natl. Acad. Sci. USA* **1990**, *87*, 6708–6712.
- [5] N. Shimoda, A. Toyoda-Yamamoto, S. Aoki, Y. Machida, *J. Biol. Chem.* **1993**, *268*, 26552–26558.
- [6] L. S. Melchers, A. J. Regensburg-Tuink, R. A. Schilperoort, P. J. Hooykaas, *Mol. Microbiol.* **1989**, *3*, 969–977.
- [7] R. G. Ankenbauer, E. W. Nester, *J. Bacteriol.* **1990**, *172*, 6442–6446.
- [8] K. M. Hess, M. W. Dudley, D. G. Lynn, R. D. Joerger, A. N. Binns, *Proc. Natl. Acad. Sci. USA* **1991**, *88*, 7854–7858.
- [9] S. C. Winans, *Mol. Microbiol.* **1991**, *5*, 2345–2350.
- [10] S. C. Winans, *Microbiol. Rev.* **1992**, *56*, 12–31.
- [11] A. M. Stock, V. L. Robinson, P. N. Goudreau, *Annu. Rev. Biochem.* **2000**, *69*, 183–215.
- [12] A. H. West, A. M. Stock, *Trends Biochem. Sci.* **2001**, *26*, 369–376.
- [13] L. N. Johnson, R. J. Lewis, *Chem. Rev.* **2001**, *101*, 2209–2242.
- [14] S. Forst, J. Delgado, M. Inouye, *Proc. Natl. Acad. Sci. USA* **1989**, *86*, 6052–6056.
- [15] J. Loh, M. Garcia, G. Stacey, *J. Bacteriol.* **1997**, *179*, 3013–3020.
- [16] K. Lee, M. W. Dudley, K. M. Hess, D. G. Lynn, R. D. Joerger, A. N. Binns, *Proc. Natl. Acad. Sci. USA* **1992**, *89*, 8666–8670.
- [17] D. Georgellis, O. Kwon, E. C. Lin, *Science* **2001**, *292*, 2314–2316.
- [18] F. Oehme, S. C. Schuster, *BMC Biochem.* **2001**, *2*, 2.
- [19] J. J. Bijlsma, E. A. Groisman, *Trends Microbiol.* **2003**, *11*, 359–366.
- [20] R. Alves, M. A. Savageau, *Mol. Microbiol.* **2003**, *48*, 25–51.
- [21] A. Oka, H. Sakai, S. Iwakoshi, *Genes Genet. Syst.* **2002**, *77*, 383–391.
- [22] Y. Wang, R. Gao, D. G. Lynn, *ChemBioChem* **2002**, *3*, 311–317.
- [23] L. M. Banta, R. D. Joerger, V. R. Howitz, A. M. Campbell, A. N. Binns, *J. Bacteriol.* **1994**, *176*, 3242–3249.
- [24] A. M. Campbell, J. B. Tok, J. Zhang, Y. Wang, M. Stein, D. G. Lynn, A. N. Binns, *Chem. Biol.* **2000**, *7*, 65–76.
- [25] B. G. McLean, E. A. Greene, P. C. Zambryski, *J. Biol. Chem.* **1994**, *269*, 2645–2651.
- [26] S. C. Winans, R. A. Kerstetter, E. W. Nester, *J. Bacteriol.* **1988**, *170*, 4047–4054.
- [27] S. C. Winans, *J. Bacteriol.* **1990**, *172*, 2433–2438.
- [28] N. J. Mantis, S. C. Winans, *J. Bacteriol.* **1992**, *174*, 1189–1196.
- [29] C. H. Chang, J. Zhu, S. C. Winans, *J. Bacteriol.* **1996**, *178*, 4710–4716.
- [30] C. H. Chang, S. C. Winans, *J. Bacteriol.* **1996**, *178*, 4717–4720.
- [31] Y. Wang, A. Mukhopadhyay, V. R. Howitz, A. N. Binns, D. G. Lynn, *Gene* **2000**, *242*, 105–114.
- [32] S. G. Jin, R. K. Prusti, T. Roitsch, R. G. Ankenbauer, E. W. Nester, *J. Bacteriol.* **1990**, *172*, 4945–4950.
- [33] S. Jin, T. Roitsch, R. G. Ankenbauer, M. P. Gordon, E. W. Nester, *J. Bacteriol.* **1990**, *172*, 525–530.
- [34] J. Zhang, L. Boone, R. Kocz, C. Zhang, A. N. Binns, D. G. Lynn, *Chem. Biol.* **2000**, *7*, 611–621.
- [35] K. Volz, *Biochemistry* **1993**, *32*, 11741–11753.
- [36] L. E. Hokin, P. S. Sastry, P. R. Galsworthy, A. Yoda, *Proc. Natl. Acad. Sci. USA* **1965**, *54*, 177–184.
- [37] G. J. Pazour, C. N. Ta, A. Das, *J. Bacteriol.* **1992**, *174*, 4169–4174.
- [38] C. H. Chang, S. C. Winans, *J. Bacteriol.* **1992**, *174*, 7033–7039.
- [39] Y. Wang, Ph.D. thesis, The University of Chicago (USA), **1999**.

- [40] G. J. Pazour, C. N. Ta, A. Das, *Proc. Natl. Acad. Sci. USA* **1991**, *88*, 6941–6945.
- [41] V. Weiss, B. Magasanik, *Proc. Natl. Acad. Sci. USA* **1988**, *85*, 8919–8923.
- [42] W. T. Peng, Y. W. Lee, E. W. Nester, *J. Bacteriol.* **1998**, *180*, 5632–5638.
- [43] F. Posas, S. M. Wurgler-Murphy, T. Maeda, E. A. Witten, T. C. Thai, H. Saito, *Cell* **1996**, *86*, 865–875.
- [44] M. A. Uhl, J. F. Miller, *EMBO J.* **1996**, *15*, 1028–1036.
- [45] A. G. Cochran, P. S. Kim, *Science* **1996**, *271*, 1113–1116.
- [46] W. Tao, C. L. Malone, A. D. Ault, R. J. Deschenes, J. S. Fassler, *Mol. Microbiol.* **2002**, *43*, 459–473.
- [47] Y. Zhu, M. Inouye, *J. Biol. Chem.* **2003**, *278*, 22812–22819.
- [48] O. Kwon, D. Georgellis, E. C. Lin, *J. Biol. Chem.* **2003**, *278*, 13192–13195.
- [49] G. A. Cangelosi, E. A. Best, G. Martinetti, E. W. Nester, *Methods Enzymol.* **1991**, *204*, 384–397.
- [50] J. H. Miller, *Experiments in Molecular Genetics*, Cold Spring Harbor Laboratory Press, Cold Spring Harbor, NY, **1972**.
- [51] B. Watson, T. C. Currier, M. P. Gordon, M. D. Chilton, E. W. Nester, *J. Bacteriol.* **1975**, *123*, 255–264.

Received: November 24, 2003